Cellular and Molecular Biology™ **44** (5), 807-826
Printed in France.

0145-5680/97
1998 Cell. mol. Biol.™

State of the Art

LASER SCANNING MICROSCOPY IN ENZYME HISTOCHEMISTRY

VISUALIZATION OF CERIUM-BASED AND DAB-BASED PRIMARY REACTION PRODUCTS OF PHOSPHATASES, OXIDASES AND PEROXIDASES BY REFLECTANCE AND TRANSMISSION LASER SCANNING MICROSCOPY

Karl-Jürgen HALBHUBER✍, Reimar KRIEG and Karsten KÖNIG

✍ Institute of Anatomy/Anatomy II, Friedrich Schiller University of Jena, Teichgraben 7, D-07743 Jena, Germany

Received March 2, 1998; Accepted June 28, 1998

***Karl-Jürgen HALBHUBER**, studied Medicine 1957-1963 at the Friedrich Schiller University of Jena, Germany. He is since 1977 Professor of Anatomy in Jena and was 1977-1990 Head of the Dept. of Histochemistry. Since 1991 he is Director of the Institute of Anatomy II Jena. Areas of interest: membranology, cerium-, enzyme- and immunohisto-chemistry, one- and multiphoton-laser-microscopy.*

***Reimar KRIEG**, studied chemistry at the University of Halle, Germany, completed the Diploma on Organic Chemistry in 1980 and worked on the field of liquid crystals. He received his doctorate in 1986 and moved into steroid chemistry at the Central Institute of Medicinal and Experimental Therapy Jena, Germany. In turn of the institutes disintegration in 1991, he began working at the Department of Organic Chemistry of the University Jena on vitamin D analogues and steroids as chiral templates. In 1996 he entered the Institute of Anatomy of the University Jena. His area of interests comprises currently chromogenic and luminogenic labels for classical and advanced laser based histochemical purposes as well as aspects of supramolecular chemistry with potential interest for diagnostic applications.*

***Karsten KÖNIG**, studied Physics at the Universities in Rostock and Jena, Germany. He received his Ph.D. on "optical detection of photosensitizers in tissue" in 1989, then his degree as an university lecturer (habilitation) on "optical micro-manupulation and two-photon excitation of living cells" in 1996. His current research in the field of biomedical optics focuses on non-linear effects of laser radiation in cells and tissues.*

Abstract - The reflectance mode of confocal laser scanning microscopy is suitable to detect cerium-based primary reaction products of oxidases (Ce^{IV}-perhydroxide) and phosphatases (Ce^{III}-hydroxy-phosphate converted into Ce^{IV}-perhydroxy-phosphate) as well as of DAB-based primary reaction products (Ni-DAB, Ni-Fe^{II}-DAB and Ce^{IV}-DAB complexes) of cytochrome C oxidase and peroxidases in vibratome, cryotome and semithin plastic sections. In combination with confocal detection 3D images with submicron spatial resolution can be obtained. Moreover, Ce^{IV}-perhydroxide, Ce^{IV}-perhydroxy-phosphate, Ce^{IV}-DAB complexes and catechol-DAB polymers are highly absorptive. Among other additives, especially stable nitroxyl radicals led to a distinct improvement of the DAB staining in terms of sensitivity and proper localization. This was proven in addition by means of blotting a horseradish peroxidase dilution series during several experiments. In sections it was easily possible to record reflectance signals and high transmission contrast at the wavelength of the exciting argon ion laser (preferentially 488 nm). The results of an imbibition study of cerium-containing model precipitates indicate that the cerium generally should be oxidized prior to observation because the index of refraction of Ce^{IV} compounds is considerably higher than that of the corresponding Ce^{III} compounds. A comparative numerical assessment of reflection intensities from reflectant parts in morphologically similar sections is possible. Confocal laser scanning microscopy offers a unique way for high resolution detection of primary histochemical reaction products being sufficiently reflective and/or absorptive. The proposed techniques may open new methodological possibilities for basic research and for medical diagnosis.

Key words: Laser scanning confocal microscopy, reflectance, transmission, enzyme histochemistry, oxidase, phosphatases, peroxidases, cerium-metal-DAB techniques, catechols, nitroxyl radicals, tetraphenylporphine

Abbreviations: CLSM: confocal laser scanning microscopy; **LSM**: laser scanning microscopy; PRP: primary cerium reaction products;

INTRODUCTION

Enzyme histochemistry represents an interdisciplinary link between biochemistry and morphology and even a bridge to molecular biology (Hardonk *et al.,* 1977; Lojda *et al.*, 1979; Meijer, 1975; Wohlrab *et al.*, 1979; Wohlrab and Gossrau, 1992). Enzymes become more and more important as histochemical tools for identification and localization of characteristic structural elements at the cellular and molecular level (Bendayan, 1981; Coulombe *et al.*, 1988; Seno *et al.*, 1989), which is of special relevance for the improvement of diagnosis in pathology as well as for the cell biological understanding of pathological processes (Hulstaert *et al.*, 1989; Rath, 1981). Last but not least, enzymes are effectively used as tracers in immunoassays (ELISA, RIA), in protein blotting, in immunocytochemistry (Cuello, 1983; Luppa *et al.*, 1986; Polak and van Noorden, 1983; Polak and Varndell, 1984) and in hybridization histochemistry (Landegent, 1987). From this wide range of applications of enzyme histochemistry it is evident that further developments in the field of catalytic enzyme demonstration techniques are of considerable interest.

Conventional one photon confocal laser scanning microscopy (CLSM) using argon ion laser (488 nm, 514 nm) and He-Ne-laser (543 nm) as irradiation sources (for reviews see Cheng and Summers, 1988; Gu and Sheppard, 1993; Pluta, 1989; Rigaut *et al.*, 1993; Shotton, 1995) offers a unique way for visualization enzymatic histochemical reaction products as well as for visualization of details of important biological structures, e.g. in chromosomes. Such reaction products are the low soluble precipitates of the enzymatically generated primary cerium reaction products (PRP) formed by phosphatases, oxidases as well as peroxidases (for reviews see Hulstaert *et al.*, 1989; van Noorden and Hulstaert, 1991; van Noorden and Frederiks, 1993; Halbhuber *et al.*, 1994). Under microscopical dark-field observation this kind of precipitates appear already as well-localized, faint, but frequently very bright, light-scattering patterns (Halbhuber *et al.*, 1994; Sebastian and Bock, 1987). However, the dark-field microscopy suffers from the drawback that portions of the tissue which are free from light-scattering material are poorly visible. CLSM, on the other hand, by using two detection channels, permits the simultaneous imaging of light-scattering and non-luminous structures and diminishes light originating from sources out of focus.

Our aim was to adapt the CLSM reflectance as well as the CLSM transmission mode to enzyme- and immunohistochemical studies of high resolution with vibratome, cryotome and semithin sections for routine purposes. The studies demonstrated the feasibility of both modes for cerium-based and DAB-based primary enzymatic reaction products (PRPs). The reflectance mode permits optical sectioning (3D image analysis). Furthermore, an attempt was made at a comparative assessment of the amount of reflective primary cerium reaction products.

REFLECTANCE-CLSM

Reflectance-CLSM has been used in histochemistry to investigate various aspects. Robinson and Batten (1989b, 1990) employed the reflectance laser scanning microscopy at first to localize cerium-based reaction products in stimulated neutrophils formed by released H_2O_2 and by lysosomal acid phosphatase activity in various cultured cells without any additional visualization steps. Robinson and Batten (1989a, 1989c) as well as the group of Turner *et al.* (1993) described the detection of DAB polymers demonstrating exogenous peroxidase activity in lysosomes of neutrophils. Lewis *et al.* (1990), Paddock *et al.* (1991) and Watanabe *et al.* (1995) demonstrated confocal reflectance images of silver grains in radioautographic specimens. Deitch *et al.* (1990a, 1990b, 1991) studied the reflectance of biocytin-filled dendrites visualized with DAB/Ni. Arnold *et al.* (1992) utilized the reflective properties of DAB polymers for

in situ hybridization experiments using digoxigenin-labelled DNA probes. Whallon *et al.* (1994) investigated the intracellular distribution of hexokinase in PC12 cells by confocal imaging of the reflection of DAB polymer formed by immunobound horseradish peroxidase. Rawlins and Shaw (1990), Rigaut *et al.* (1993) and Linares-Cruz *et al.* (1994, 1995) applied the method using an *in situ* hybridization protocol for the detection of riboprobes labelled by 1 nm-5 nm (also silver enhanced) colloidal gold particles. Kazama *et al.* (1994) and Neri *et al.* (1997) described an immunohistochemical and enzyme-histochemical double staining utilizing the reflective properties of colloidal gold particles as well as lead phosphate precipitates in the laser scanning confocal microscope. Ploton *et al.* (1994) described the visualization of silver dots on proteins of the nucleolar organizer regions (Ag-NOR proteins) employing the confocal laser scanning reflectance mode. Duschner (1995) proposed the use of the CLSM to estimate changes in the dental enamelum of humans. In recent studies, Ito and Otsuki (1998) localized apoptotic cells *in situ* as well as specific chromosome regions, detected by the reflectance from anti-digoxigenin antibody-immunogold-silver complexes.

Our experimental results demonstrate, that the highest reflectance intensities using an argon ion laser (488 nm) are accompanied with PRP of oxidases consisting of Ce^{IV}-perhydroxide (Ce^{IV}-OOH) and Ce^{IV}-hydroxide (Ce^{IV}-OH; Fig. 1). Considerable reflectance intensity was also observed with Ce^{IV}-perhydroxy-phosphate-based (Ce^{IV}-PHP, Fig. 2) PRP. In general, in sections Ce^{III}-based PRPs gave much lesser reflectance signals (Fig. 3). These observations were confirmed in model preparations, which showed that generally Ce^{IV} compounds were higher reflective compared with Ce^{III} reaction products. The highest reflectance being observed in case of Ce^{IV}-OOH and Ce^{IV}-OH as well. The Ce^{IV}-phosphate containing compounds were considerably less reflective than Ce^{IV}-hydroxides (Halbhuber *et al.*, 1996).

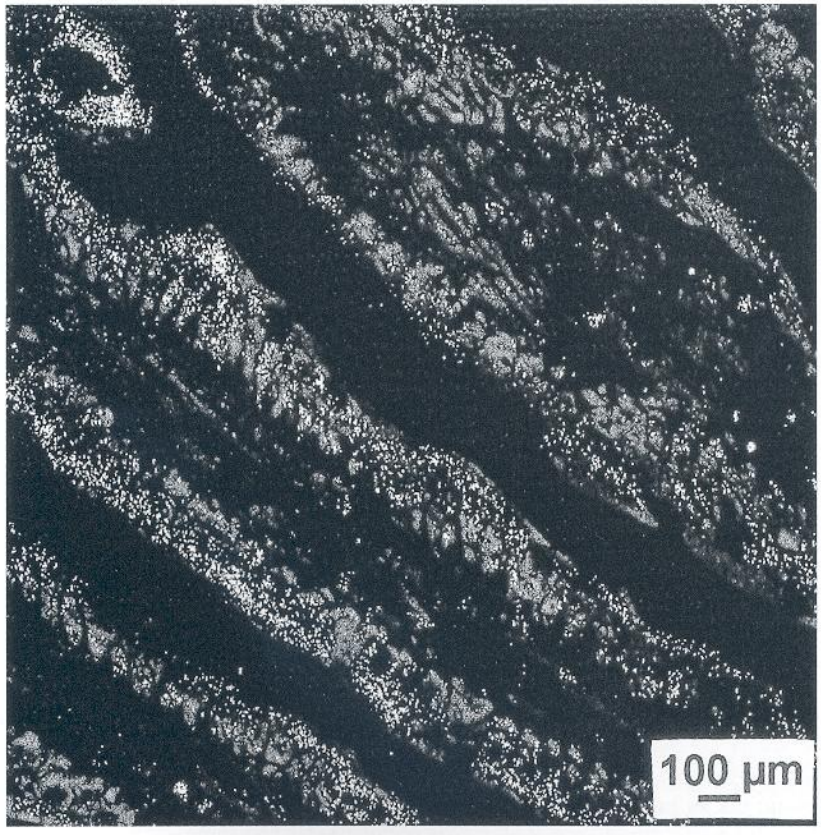

Fig. 1 *D-proline oxidase activity in peroxisomes, enterocytes, intestine, rat.* Reflectance of reoxidized PRP (Ce^{IV}-OOH), autofluorescence/reflectance overlay, cryotome section.

In account with the formulas of Fresnel, governing the amount of reflection (reflectance) with respect to the entrance angle and polarization, and the Snellius' law, it is obvious, that the reflection behavior of a given cerium-based PRP should be directly related to its index of refraction. This was confirmed by our gross imbibition study: High reflectance of a PRP in histochemical preparations corresponds to a high index of refraction of model precipitates of which the PRP is assumed to consist of (Halbhuber *et al.*, 1996). With respect to the imaging of H_2O_2-generating oxidases, it was observed that the Ce^{III} ions in two steps capture enzymatically liberated H_2O_2 to form Ce^{IV}-OOH as the true PRP. However, the Ce^{IV}-OOH is regarded to oxidize subsequently Ce^{III} ions which are present in the incubation medium in form of dextrane-Ce^{III} complexes, resulting in a reduction of the Ce^{IV}-OOH and its conversion into Ce^{IV}-OH (Halbhuber *et al.*, 1991, 1994). Therefore, in order to achieve optimized reflection intensities, the latter compound should be reoxidized into Ce^{IV}-OOH with H_2O_2 prior to CLSM microscopy. Irrespective of the high index of refraction of Ce^{IV}-OH, the reflec-

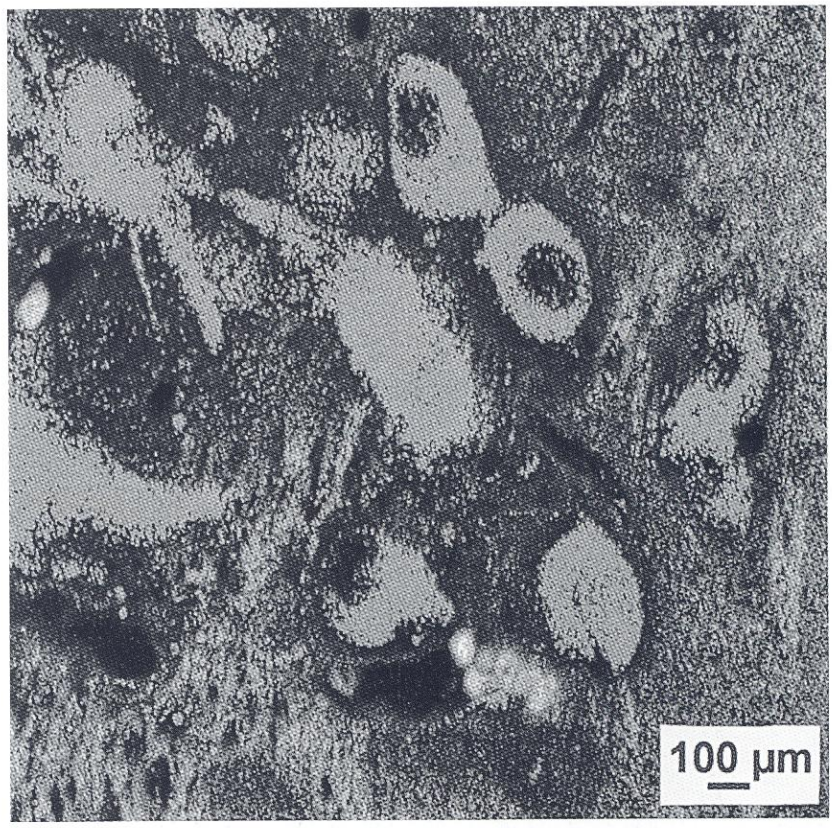

Fig. 3 *Immunobound alkaline phosphatase cerium method* (antivasopressin-APAAP), *nucleus supraopticus, rat.* Reflectance/autofluorescence overlay of PRP (Ce^{III}-hydroxy-phosphate) without any reoxidation. Cryotome section.

page 811 top

Fig. 2 *Alkaline phosphatase activity in myoepithelial cells of the submandibular gland, rat.* Reflectance of reoxidized PRP (Ce^{IV}-perhydroxy-phosphate) red, autofluorescence green. False color overlay. Cryotome section.

page 811 bottom

Fig. 6 *Immunobound peroxidase activity. Reflectance/transmission false color overlays.* Semithin Epon plastic sections, rat. **a**) Apoptotic nuclei in intestinal villis (tips, stroma cells with yellow reflectance signals). Non-apoptotic nuclei gave very weak or no reflection images. Ce^{IV}-DAB polymers; **b**) The same as in **a**, however catechol-DAB final reaction products; **c**) Neurohypophysis, rat. Demonstration of vasopressin in Herring bodies. Ce^{IV}-DAB reaction products as in **a**. **d**) The same as in **c**. Catechol-DAB reaction products.

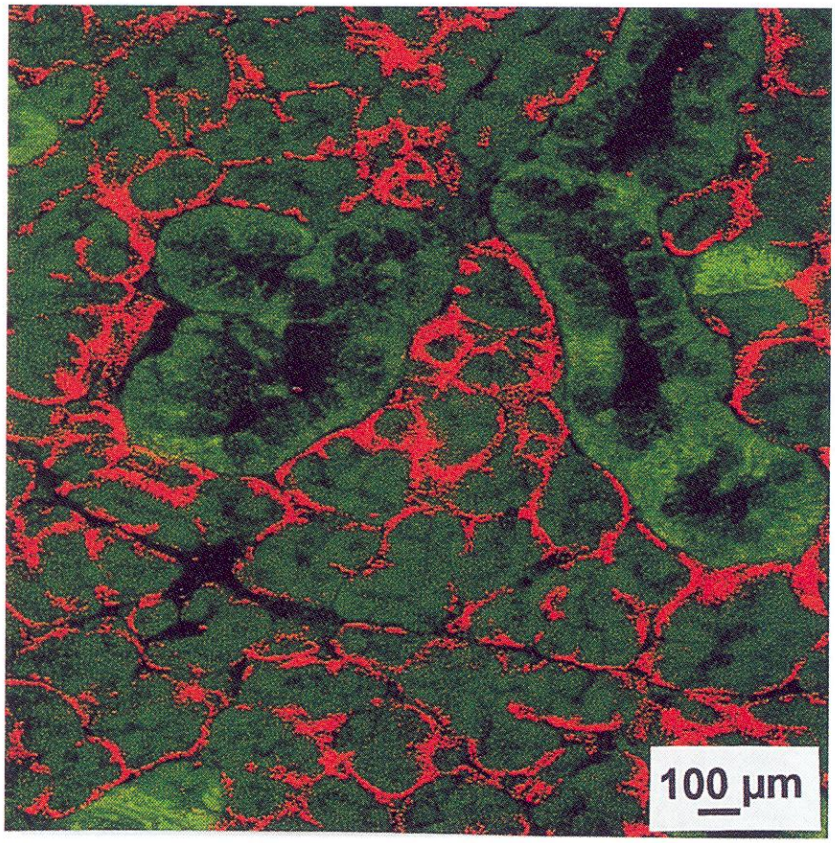

2

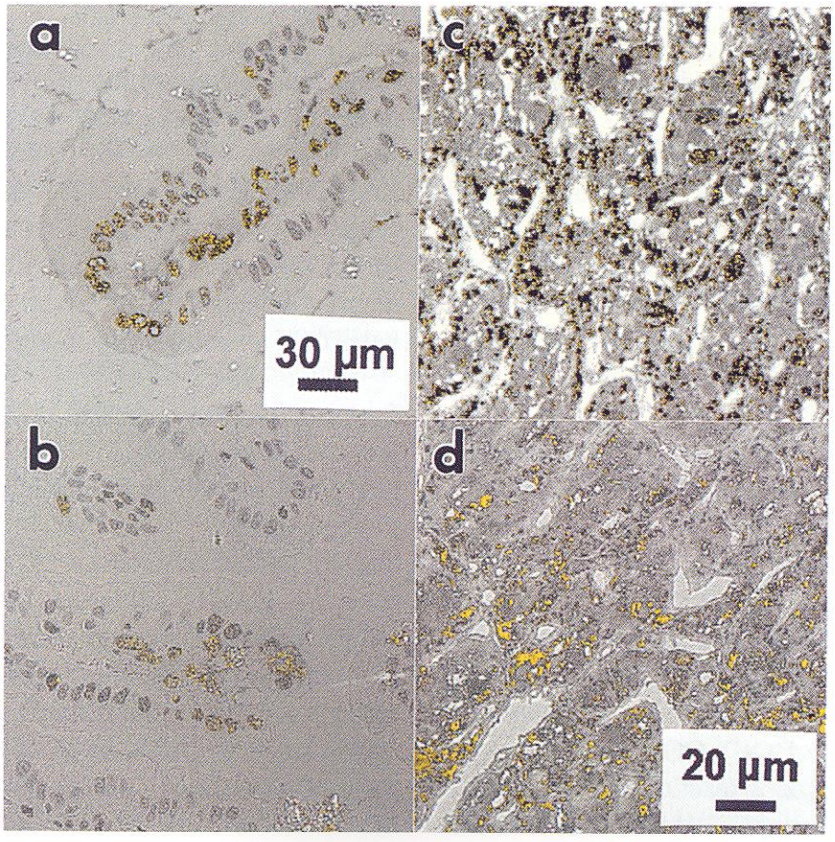

6

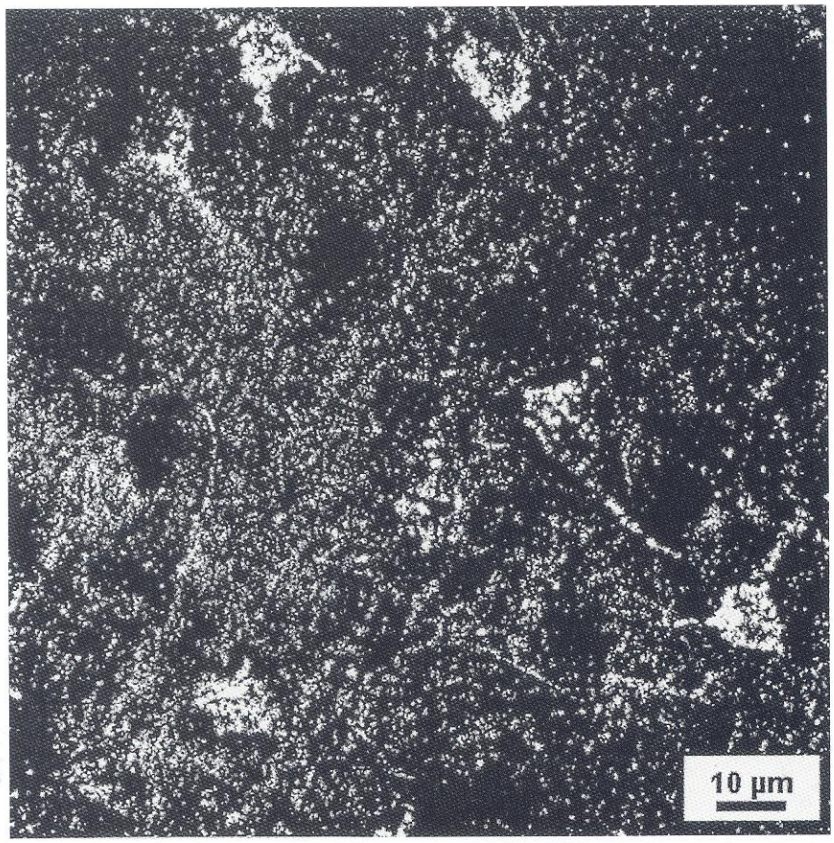

Fig. 4 *Cerebral cortex, rat.* Horseradish peroxidase tracing of neurons. Reflectance of Ni-Fe^{II}-DAB reaction product. Note the excellent visualization of nanometer-sized PRP.

tance signals of this compound still were significantly lower than that of Ce^{IV}-OOH.

Excellent reflection intensities were also yielded with metal-DAB complexes as demonstrated with the enzymatically generated PRP of immunobound and endogenous peroxidase activities as well as of oxidase activities (COX, H_2O_2-generating oxidases). Beside Ni-DAB complexes (Halbhuber *et al.,* 1996) especially Ni-Fe-DAB and Ce^{IV}-DAB complexes are highly reflective (Figs. 4, 5b, 6b) even in semithin sections when viewed under non-confocal conditions. Strand breaks of DNA in apoptotic nuclei labelled by a TUNEL-technique (Aschoff and Jirikowski, 1997) using the metal-DAB protocol revealed in such sections significant higher reflection intensivities than non-apoptotic nuclei (Fig. 6a). Employing these results, a further amplification of the reflection signals of Ce^{IV}-OOH or Ce^{IV}-perhydroxy-phosphate enzymatic reaction products is possible (Fig. 7). In this special case, the oxidized cerium-incubated sections should be postincubated in metal-DAB media for 10-30 min. at 20°C.

Regarding the use of Ni-Fe^{II}-DAB solutions, it is absolutely recommended that the incubation time should be restricted to 15-20 min. to avoid the formation of black-blue colored reaction products. The latter may absorb reflection signals remarkably.

In case of application of metal additives in the presence of chromogenic 1,2-dinucleophiles as DAB (and the below discussed catechols), the occurrence of metal chelates with the chromogen and subsequently related intramolecular redox- and catalytic processes must be taken into account too. Recently were described transition metal complexes of 1,2-bezoquinones and their intramolecular electron transition processes (Gütlich and Dei, 1997). In electron spin resonance studies the DAB polymerization product showed a large "free spin type" of signal while the monomer did not (Hiraoka *et al.*, 1986).

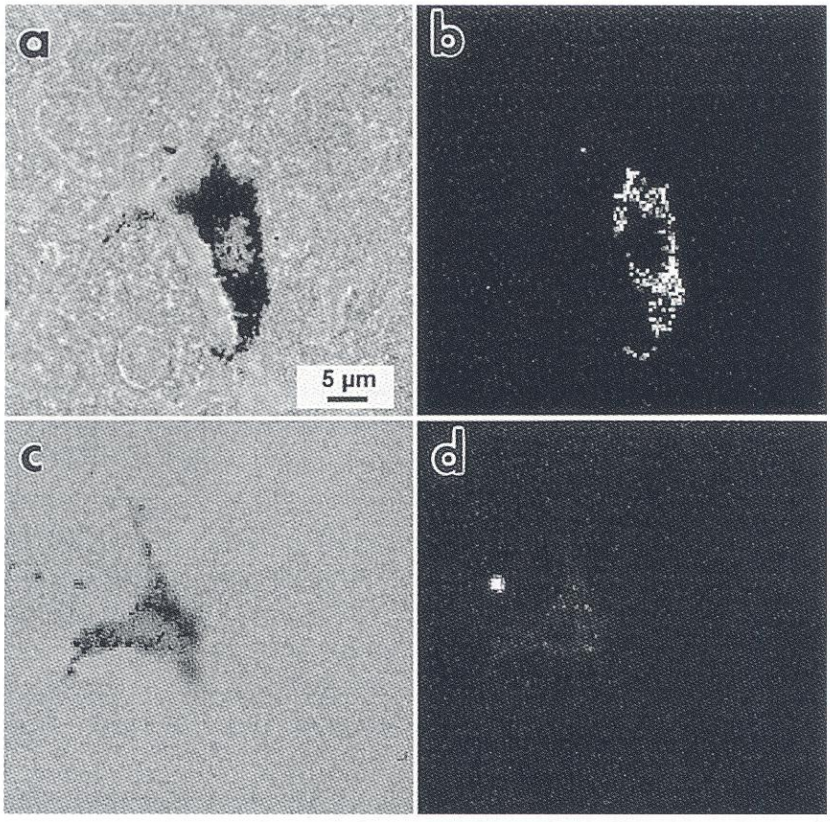

Fig. 5 *Endogenous peroxidase activity in lysosomes of liver macrophages, rat.* Transmission and reflection images of PRPs, vibratome sections. **a**) Transmission image; **b**) confocal reflectance image of Ce^{IV}-DAB polymers; **c**) transmission image; **d**) reflectance image of Karnovsky not metal containing DAB polymers. The not metal DAB reaction products provide evidently lower transmission contrast and lower reflectance intensity than the Ce^{IV} containing DAB products.

This means, that highly reactive free radicals are formed during DAB polymerization capable of binding metals to form metal-DAB polymerization products. The presence of metals in these compound was confirmed by energy dispersive X-ray analysis (EDAX) of metal-DAB polymers (Hiraoka *et al.*, 1986). The metal-DAB polymerization products are more stable during ultra violet light irradiation than the not metal containing DAB polymers. This is further supported by their low solubility and high density (DAB polymer: d=1.474, Pt-DAB polymer: d=2.156; Hiraoka 1992, personal communication).

The following metal-DAB incubation media are proposed:

1. Ni-Fe^{II}-DAB

50 mM TRIS-HCl buffer, pH 8.0
0.5% $NiSO_4$
0.01% Ammonium-Fe^{II}-sulphate
0.02% DAB
(addition of 0.005% TEMPO in
0.1 ml of THF is possible)
0.005% H_2O_2

2. Ce^{III}-DAB

0,1 M Sodium acetate buffer, pH 5.0
(with or without dextrane T70 which
inhibits the formation
of Ce-DAB precipitates in
the medium)
0.02% DAB
(addition of 0.005% TEMPO in 0.1 ml
of THF is possible) 0.005% H_2O_2

The incubation lasted about 10-30 min. at 20°C.

A quantitative assessment of the reflecting power and its correlation with the enzymatic activity of cerium- or DAB-based precipitates meets with several difficulties. First of all, the combined effect of backscattering and absorption by the precipitates causes considerable attenuation of the illuminating beam with increasing depth of the plane of focus. This results in a more or less pronounced decrease of reflectance within the section. Moreover, the dependence of the reflectance on the depth of the plane of focus implies the necessity of strictly controlling the distance of the plane to be imaged from the surface of the section. This may be difficult in view of thickness and irregularities of the most routine sections as well as by diffusion behavior of the incubation constituents. Therefore, quantifying the amount of precipitates simply by summing up the light backscattered from a distinct layer within a histological section will in general be an unreliable procedure. Under restricted conditions, however, such as with objects containing reflecting PRP only in a sufficiently fine pattern, the method may be of interest for comparative purpose (Halbhuber *et al.*, 1996).

In table 1 the ratios Ce^{IV}/Ce^{III} of reflectance signals R of different organs are shown to demonstrate in principle the feasibility of a quantitative comparison of morphologically similar reflectance patterns indicating different alkaline phosphatase activities in different tissues: Ce^{IV}-perhydroxy-phosphate is in its reflectance clearly superior to Ce^{III}-hydroxy-phosphate (22.7 ileum and 83.9 gl. seminalis). The surprising high variation of the ratios is difficult to explain. Possibly, the observed variability is related to different growth conditions of the Ce^{III}-hydroxy-phosphate or/and Ce^{IV}-perhydroxy-phosphate precipitates, and the local surrounding conditions

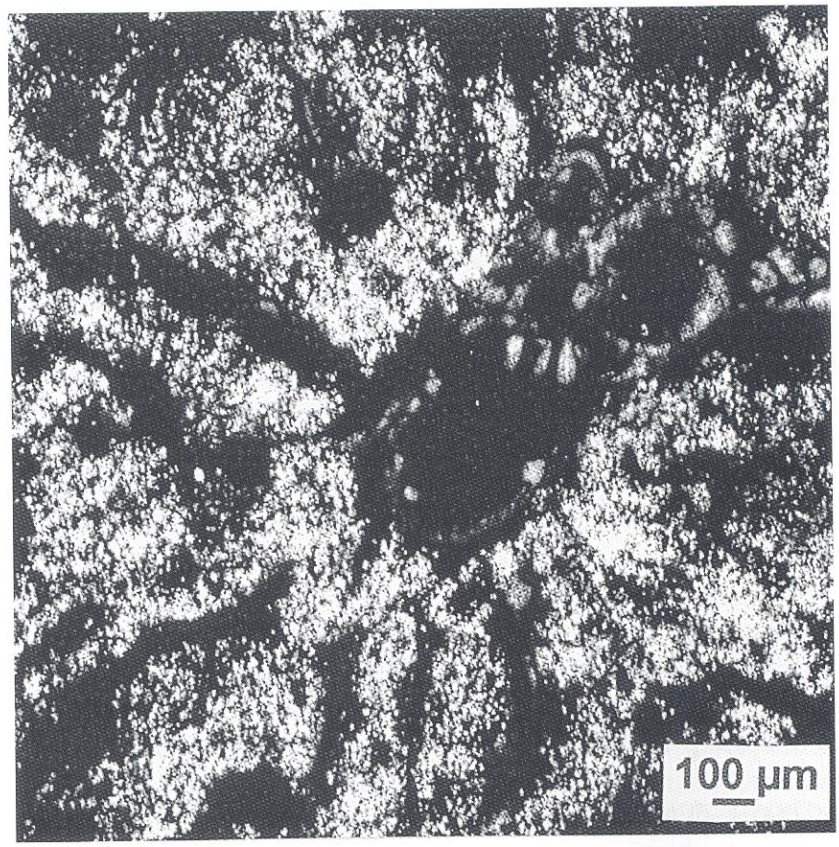

Fig. 7 *Uricase activity, liver, rat. Autofluorescence/reflectance overlay of reoxidized PRP* (Ce^{IV}-OOH) *after amplification with Ni-Fe^{II}-DAB polymers.* Cryotome sections. Note the strongly increased reflectance compared with the non-amplified PRP as seen in fig. 1.

Table 1 *Comparison of ratios of reflectance signals R of Ce^{IV}-perhydroxy-phosphate and Ce^{III}-hydroxy-phosphate as the reaction product of alkaline phosphatase activity in cryotome sections of several organs*

Organ	R_{CeIV}/R_{CeIII}
Ileum[1], control	22.7 ± 1.2
Ileum[1], 95' after NaCl stress	43.8 ± 2.2
Cerebrum[2]	62.3 ± 9.2
Gl. seminalis[3]	83.9 ± 16.2

[1]Brush border of enterocytes (Ott, 1998); [2]capillaries in the cerebral cortex; [3]connective tissue

which may vary appreciably with the macromolecular components of biostructures in the vicinity of the enzyme sites.

The quantitation of specific reflectance may be interfered by unspecific background reflectance too. It may originate both from non-specific precipitate and from tissue reflectance due to local inhomogeneities of the index of refraction below the resolution limit. Non-precipitated, electrovalently bound Ce^{III} ions could, in cases where a post-oxidizing treatment with H_2O_2 had been included, give rise to background reflectance unrelated to any enzyme activity by formation of Ce^{IV}-OOH. For this reason, the treatment with a Ce^{III}-chelating agent like EDTA (ethylenediaminetetraacetic acid) and DTPA (diethylenetriaminepentaacetic acid) is necessary. In studies of other authors, complexing of lanthanides was carried out in a similar manner for other purposes, e.g. for fluorescence sensitization (Abubaker *et al.*, 1993), in flow cytometry (Condreau *et al.*, 1994) and for chelate labeling in histochemistry (Seveus *et al.*, 1992). For our purposes EGTA (ethyleneglycol-*bis*-(β-aminoethyl)ether) was most convenient to clear selectively Ce^{III} ions whereas EDTA treatment led to considerable loss of specific PRP.

The main contribution to the non-specific reflectance can obviously derived from the optical inhomogeneity of the tissue. In order to minimize this background, proper matching of the mounting medium and the tissue is essential, a fact well known from dark field microscopy (Sebastian and Bock, 1987). According to our work, Canada balsam (n=1.520) was found to render better matching than Entellan (n=1.495). Another source of tissue background was found in the customary air-drying of fresh cryotome sections. Therefore, the fresh cryotome sections were directly transferred into the fixative without air-drying at all (Halbhuber *et al.*, 1996).

Nonetheless, optical inhomogeneities can also provide suitable informations reflecting structural properties in Giemsa-stained human chromosomes. In fig. 8 is clearly demonstrated a reflectance banding pattern which corresponds negatively to the Giemsa-banding pattern as seen with the transmission mode ("negative banding"). It is interesting to note, that this banding pattern only was observed after standard-preparation and Giemsa-staining of chromosomes. It was abolished completely when the Giemsa-staining was omitted. The reason of this phenomenon is still unclear. It seems, that after binding of Giemsa-dyes supramolecular arrangements of DNA-protein complexes are induced, which are strongly reflective. It is suggested that the reflectance signals in the Giemsa-stained bands may obviously absorbed. Further experiments are necessary to understand the molecular basis for the type of "dye induced" chromosomal reflectance banding pattern.

In summary, the reflectance method provides a valuable tool for detecting of distribution patterns of enzymatic reaction products with inherent high-contrast imaging even in cases of weak enzymatic activity in relative thick material (10-15 µm cryotome and paraffin sections, 30-60 µm thick vibratome sections). With the restrictions discussed above, it is possible to compare quantitatively the variations of such patterns caused by pathological deviations or experimental manipulations. In contrast to non-confocally working, dark field methods and their inherent optical disturbances caused by light-scattering structures out of focus reflectance, confocal laser microscopy offers a tool

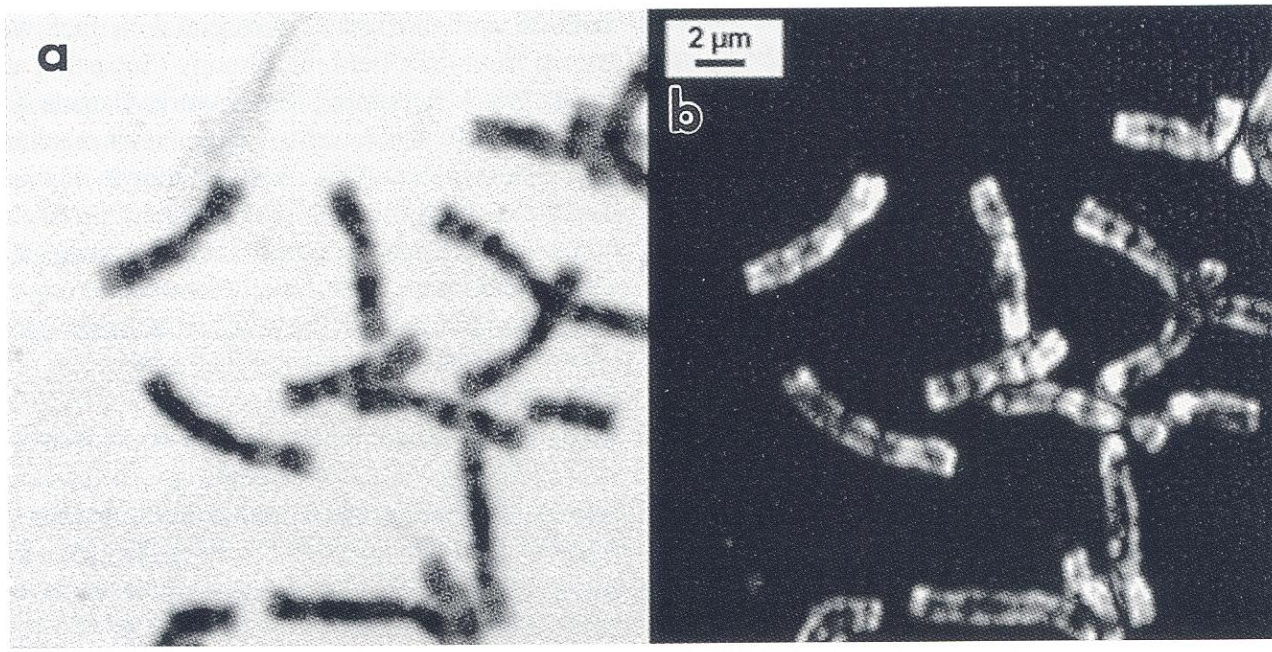

Fig. 8 *Isolated metaphase human chromosomes* (lymphocytes, Giemsa-stained). **a**) Transmission image with "positive banding pattern"; **b**) reflectance image with "negative banding pattern"

for the photometric determination of the amount of light-scattering reaction products in a defined layer within the object. Nevertheless, semithin sections plastic (0.5-1.0 µm) should be exclusively viewed in the reflectance mode under non-confocal conditions, because the yield of specific reflectance signals is significantly increased whereas non-specific background signals remain very low. In this special case the "signal to noise ratio" seems to be maximally due to the minimal contribution of non-reactive structures to the background reflectance pattern.

TRANSMISSION-LSM

Cerium-^{IV} as well as DAB-based PRPs of oxidases and phosphatases are more or less yellow-brown or brown tinged. Therefore, these group of compounds is highly absorptive for laser light at 488 nm. The polymer Ce^{IV}-DAB complex is similarly brown, but of higher contrast in comparison with DAB polymers generated in the absence of metal additives. Thus, cerium ions were used for contrast amplification of the DAB method especially for the laser transmission contrast enhancement. It is presumed that in case of Ce-DAB protocol during incubation Ce^{III} is converted into the yellow-brown colored Ce^{IV} to form Ce^{IV}-DAB polymer reaction products. From this point of view, the transmission contrast of the Ce^{IV}-DAB polymers is due to the high absorbance of the Ce^{IV} cations as well as to the dark brown tinction of the modified DAB polymers. Polymerization and precipitation of DAB is in the presence of cerium compounds much quicker as well as more precise than without cerium. In general, precipitates of Ce^{IV}-DAB are smaller and the risk of diffusion artefacts is reduced, which will

page 817 top
Fig. 9 *Peroxisomal D-valine oxidase activity, kidney, rat.* Transmission images of **a**) reoxidized PRP (Ce^{IV}-OOH); **b**) Ce^{IV}-DAB amplified PRP in cryotome sections; **c**) as in **a**; **d**) as in **b** in semithin plastic sections.

page 817 bottom
Fig. 10 *Immunobound peroxidase activity, cytokeratin, human ureter.* Transmission image of Ce^{IV}-DAB polymers as PRP. Paraffin section.

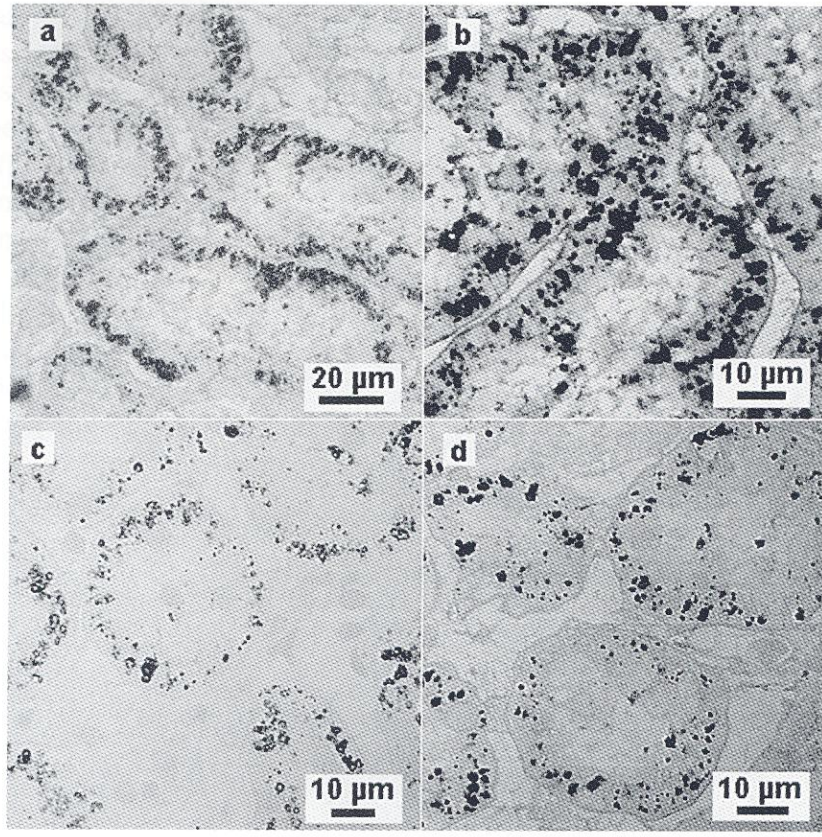

9

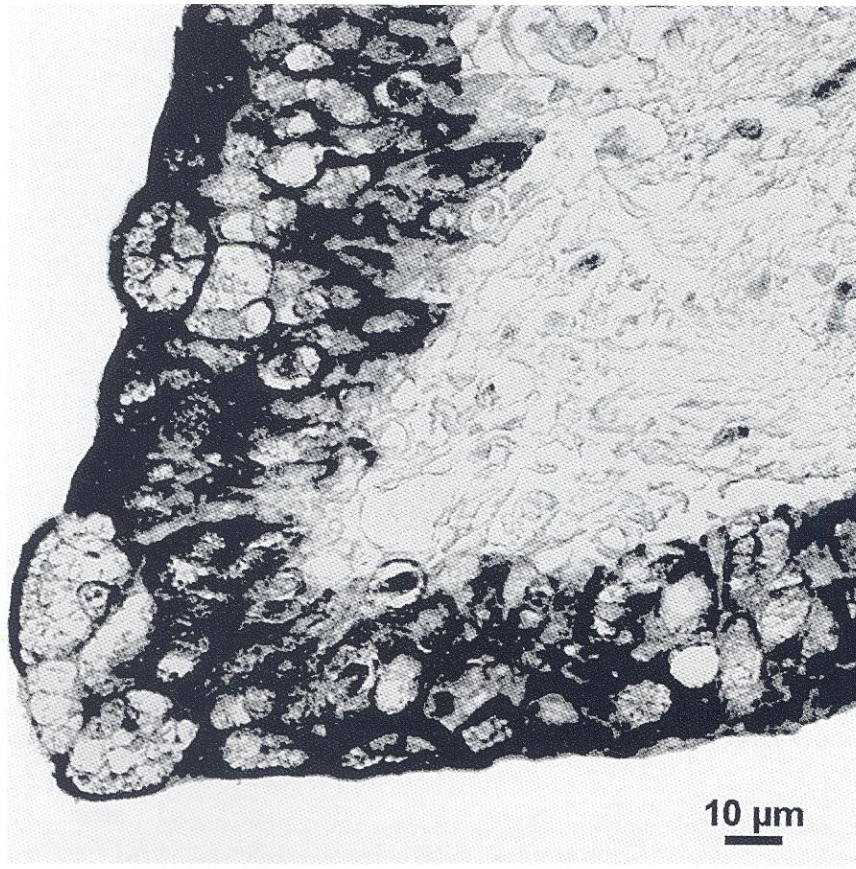

10

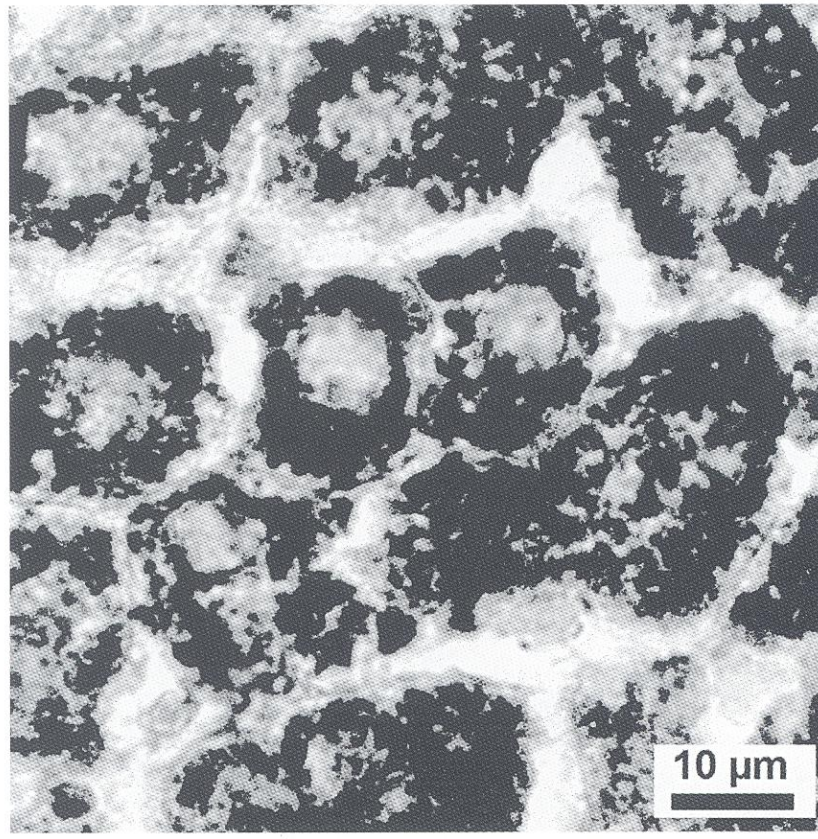

11

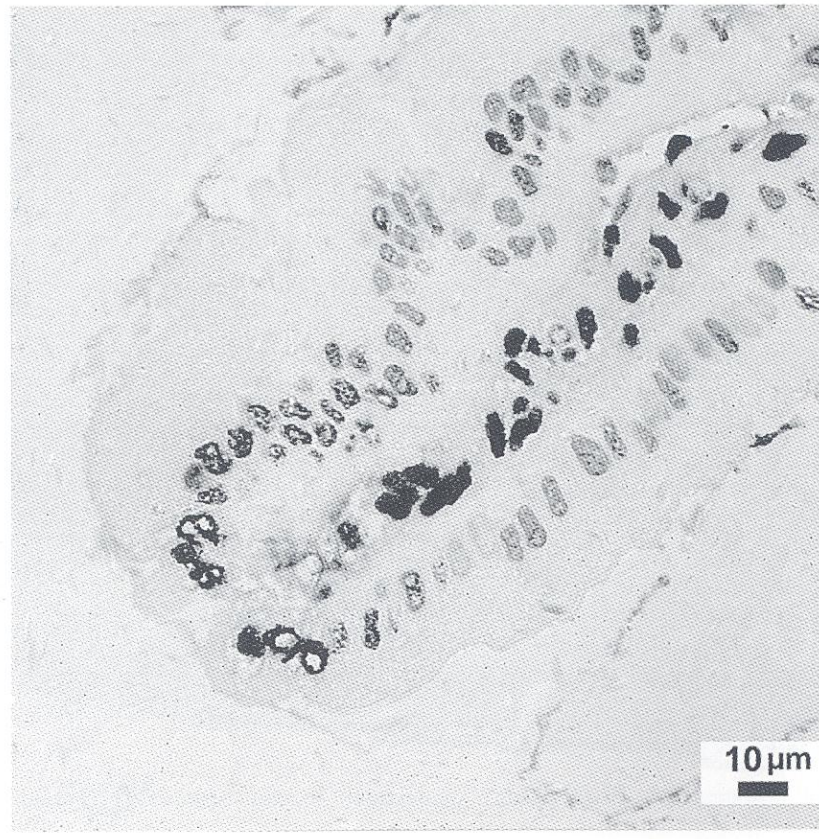

12

enhance the lateral resolution considerably. The figs. 9 to 12 demonstrate the efficiency of cerium as a means of contrast enhancement in oxidase and peroxidase histochemistry. In contrast to this the blue tinged Ni or Ni-Fe^{II} DAB polymerization products gave much lower transmission contrast than the Ce^{IV}-DAB counterparts (Fig. 13).

The factors controlling the interaction of reactive DAB intermediates during the staining oxidation cascade, critically depend on the used multicomponent systems. The rate and orientation of the interacting constituents obviously depends on the relative reactivity of the competiting intermediates. The above discussed influence of cerium additives on the oxidative DAB staining reaction should be due mainly to three contributions:

1) The well known metal catalytic effect on the DAB oxidation,

2) the oxidation-reduction potential of the enzymatic system in relation to that of the reductants, and that of the reductants among one another in a multicomponent system. The latter are represented here by competing Ce^{iV}-OOH, Ce^{IV} and Ce^{III} species and their complexes.

3) Physico-chemical effects due to the occurrence of highly charged metal cations and metal containing intermediates and their influence onto the pre-

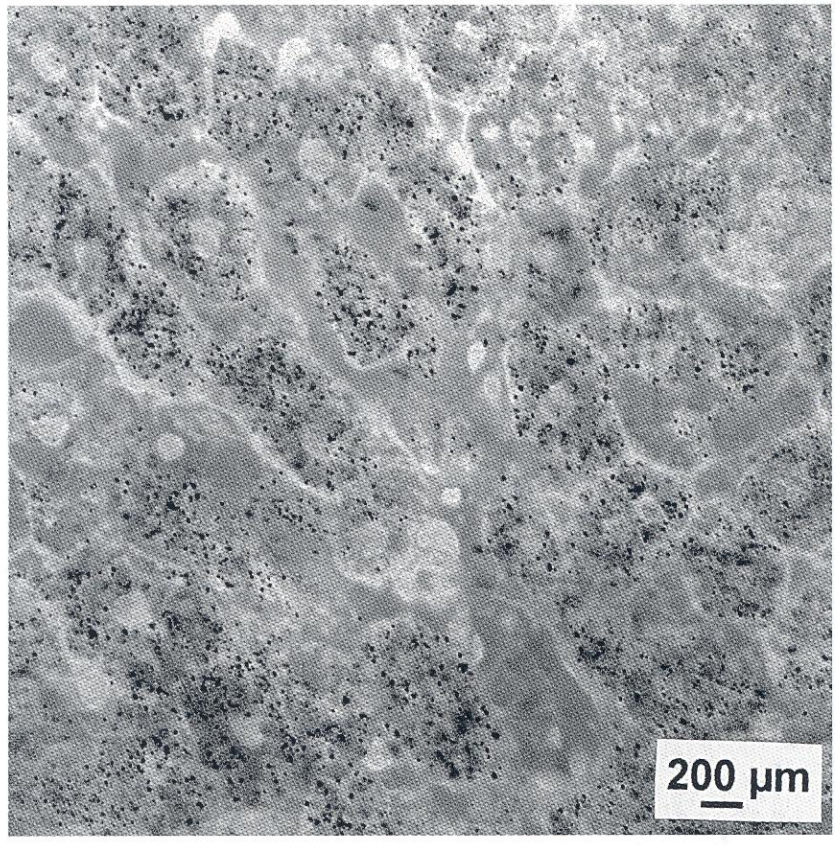

Fig. 13 *D-valine oxidase activity, liver, rat.* Transmission image of Ni-Fe^{II} DAB-amplified primary PRP Ce^{IV}-OOH. Note the low transmission contrast compared with Ce^{IV}-DAB complexes. Cryotome section.

page 818 top
Fig. 11 *Monoaminooxidase activity, liver, rat.* Ce^{IV}-OOH-based PRP amplified with Ce^{IV}-DAB. Transmission image. Note the high resolution and the high contrast imaging of the mitochondria. Cryotome section.

page 818 bottom
Fig. 12 *Apoptotic nuclei of enterocytes, intestine, rat.* TUNEL-reaction. Immunobound peroxidase activity, transmission image of Ce^{IV}-DAB-based PRPs. Semithin Epon plastic section.

Table 2 *SDS-polyacrylamide minigel electrophoresis and blotting onto nitrocellulose of a HRP dilution series ($1 : 2^n$, starting concentration 10 mg/ml; blots were incubated in 10 ml of the corresponding buffer)**

No	Reactants	final stained Dilution	Buffer (pH) Color of Stain
1	5 mg of DAB, 0.1 ml of 1% H_2O_2 [a]	1 : 512	50 mM TRIS (7.5) brown
2	as **1** +15 mM $NiSO_4$	1 : 1024	100 mM HEPES (8.0) strong blue-violet [b]
3	0.05% DAB, 0.01% H_2O_2 0.5 mg catechol	1 : 128	50 mM TRIS (7.6) brown
4	as **3** but only 0.0005% H_2O_2	1 : 256	as **3** brown
5	as **3** + 1 mM $NiSO_4$, 0.6 mM $CoCl_2$ [c]	1 : 512	10 mM phosphate-b (7.5) strongly blue-grey
6	as **5** but catechol has been omitted	1 : 256	as **5** reddish violet
7	0.02% DAB, 0.005% H_2O_2 0.5% $CeCl_3$	1 : 512	100 mM acetate-b (5.0) brown
8	as **7** + 1.5 mg catechol	1 : 256	as **7** dark brown
9	0.015% DAB, 0.005% H_2O_2 2% $NiSO_4$	1 : 64	100 mM PIPES (6.5) blue-grey
10	as **9** + 0.5% $CeCl_3$	1 : 64	as **9** pale blue grey
11	0.01% DAB, 0.005% H_2O_2 , 0.1% catechol, 0.05% p-phenylendiamine, 0.5% $CeCl_3$	1 : 512	100 mM acetate-b (5.0) dark red-brown
12	0.01% DAB, 0.01% H_2O_2 , 0.005% catechol, 0.02% 2,7'-diaminofluorene	1 : 512	25 mM TRIS (7.5) strongly red-brown [b]
13	as **12** + 0.005% TEMPO	1 : 512	25 mM TRIS (7.5) strongly brown [b]
14	0.015% DAB, 0.01% H_2O_2 0.1% $NiSO_4$	1 : 1024	100 mM HEPES (7.8) dark blue violet [b]
15	0.015% DAB, 0.005% H_2O_2, 0.1% $NiSO_4$	1 : 1024	100 mM HEPES (8.0) strongly blue violet [b]
16	as **15** + 0.005% TEMPO	1 : 1024 - 2048	as **15** dark blue violet [b, d]
17	0.02% DAB, 0.005% H_2O_2, 0.005% 4-carboxy-TEMPO	1 : 1024	100 mM HEPES (8.0) dark brown [b]
18	as **17** + 0.1% $NiSO_4$	1 : 1024	as **17** dark blue violet [b]
19	0.03% DAB, 0.005% H_2O_2, 0.01% *meso*-tetraphenylporphine, 0.15% $NiSO_4$	1 : 256 (dry blot: 1 : 2048)	100 mM HEPES (8.0) dark blue violet [b, d]
20	as **19**, but instead of $NiSO_4$ 0.15% $CoCl_2$	1 : 1024 (dry blot: 1 : 2048)	as **19** dark blue grey [e]
21	as **19**, but instead of 0.15% $NiSO_4$: 0.05% $CoCl_2$ and 0.005% $CuSO_4$	1 : 1024 (dry blot: 1 : 2048)	as **19** dark blue violet
22	as **17** + 0.05% $NiSO_4$	1 : 2048	as **17** brown
23	0.02% DAB, 0.005% H_2O_2, 0.005% TEMPO, 0.05% $NiSO_4$	1 : 2048 - 4096	100 mM HEPES (8.0) strongly blue violet [b]

cipitation behavior (restraining of colloids) and onto the precipitate itself by metal incorporation (reflectance, refraction index, color, electron density).

In mind, that the oxidative staining cascade represents a complex interplay of synergetic and competitive radicalic reaction pathways, we investigated the influence of some further additives onto the staining efficiency: Further redox active transition metals, aromatics on principle capable of undergoing coupling reactions (catechols, 2,7'-diaminofluorene) and radical mediators (stable nitroxyl radicals as e.g. 2,2,6,6-tetramethyl-piperidine-1-oxyl - TEMPO and *meso*-tetraphenylporphine).

In this experiments, low valent transition metals as e.g. Co^{2+}, Ni^{2+}, Mn^{2+} or Fe^{2+} frequently led to increased staining sensitivity and precipitation speed, whereas especially in presence of Fe^{3+}-salts the staining reaction frequently failed (radical trapping or other inhibitory effects).

Depending on the metal, a nucleophilic addition of hydrogen peroxide at the free or chelated metal center is assumed to lead to reactive oxidizing species mainly in two ways:
1) *Via* furnishing of more or less stable metal intermediates, e.g. as above discussed for Ce^{IV}-OOH. Those intermediates may be useful as "deposition tools' for enzymatic activity as examplarified here by the Ce-PRP technique. Recently, in non-enzymatic model experiments, the relative reactivities of some transition metal alkyl-hydroperoxides were discussed in mechanistically considerations and alternatively peroxo-metal or oxo-metal pathways were distinguished (Lempers *et al.*, 1998).
2) In case of less stable metal-hydrogen peroxide intermediates, the fast occurrence of free radicals is reasonable, as e.g. hydroxy radicals capable of hydroxylating (oxidizing) aromatic substrates too. This type of reaction is represented by the Fe^{II}-related *Fenton* chemistry (also the *Haber-Weiss* reaction, see e.g.: Brook *et al.*, 1982) and their modifications by chelators, which can be involved into the redox events too (Van der Zee *et al.*, 1993).

The staining sensitivity of DAB in the presence of different additives and under different reaction conditions was estimated by means of electroblotting (details and results see Table 2). After gel electrophoresis, a dilution series of horseradish peroxidase was blotted onto nitrocellulose membranes and incubated with the appropriate additives (catechol, 3,5-*di-tert*-butyl-catechol, the stable nitroxyl radicals TEMPO and 4-carboxy-TEMPO, *meso*-tetraphenyl-porphine, 2,7'-diamino-fluorene). A selection of our optimization effords is outlined in table 2 verifying the staining sensitivities in the presence of the exemplarily chosen metal salts and additives concerning the not modified DAB protocol.

Legend Table 2
[a]Karnovsky method; [b]very fast and neat staining; [c]Adams protocol; [d]very sharp band patterns; [e]weekly stained background; *Experimental details: Gels were cast by established procedures (Doucet and Trifaro, 1988; Doucet *et al.*, 1990) and run according to the respective manifacturer's instructions (20 min. at 60 V, than 40 min. at 150 V). The separating minigel composition consisted of 10% acrylamide, 0.1% N,N-methylene-*bis*-acrylamide (ratio 1 : 100) in 0.4% sodiumdodecylsulfate (SDS), 5% glycerol, 200 mM TRIS buffer and 100 mM glycine (final pH 6.7, no pH adjustment), polymerization with 0.15% ammonium persulfate and 0.05% N,N,N',N'-tetramethylenediamine (TEMED). Native semidry blotting onto nitrocellulose (0.45 mm, Schleicher & Schuell) was performed according to Pharmacia LKB Biotechnology (S 751 82 Uppsala, Sweden) instructrion no. SD RE-072 at 0.8 mA/cm^2. HRP-dilution series: starting concentration 10 mg/ml electrophorese buffer, dilution 1 : 2^n, each applied volume 3 ml. Staining for peroxidase activities: Subsequently to the transfer, the NC-membranes were preequilibrated for 5 min. in 20 mM TRIS-buffer (pH 5.8) containing 137 mM NaCl and 0.1% of Tween 20. Incubation was performed at room temperature in 10 ml of the corresponding buffer (Table 2). The staining reaction was stopped after a dark stain has been developed or at the beginning of background staining (at least 3 min.), by rinsing again in 20 mM TRIS buffer (pH 5.8) containing 137 mM NaCl and 0.1% of Tween 20. The wet blots were instantly evaluated and photographed to maintain maximum constrast. The results are given in table 2. All reagents were purchased from Sigma excepted the *meso*-tetraphenylporphine (STREM Chem.).

In general, the wide-ranging reactivity of assumed quinoid intermediates toward O, N or S nucleophiles is potentially relevant for the efficiency of the gradually occurring oxidative polycondenzation cascade *via* radical intermediates. It is also relevant for the coupling of additives and for cross linking processes with the environment.

In general, during a two-electron oxidizing process, 1,2- (e.g. DAB) and 1,4-diamines (e.g. p-phenylendiamine) as well as phenols (e.g. catechols) are regarded to lead to quinoide key intermediates capable for further intermolecular self- (e.g. DAB) or hetero-coupling (e.g. Hanker/Yates reagent) steps.

Consequently, phenols as well as amines could behave in binary chromogenic DAB mixtures as efficient couplers leading to an enhanced enzyme detection sensitivity or to modified reaction products, or, on the other hand, to intermediates of only low reactivity finally slowing down or braking down the overall oxidation cascade (inhibitory effect).

Thus, the addition of 0.005% of catechol (1,2,-dihydroxybenzene) to a standard DAB protocol led to a distinct increase of the staining sensitivity and resolution of the low soluble, reddish-brown tinged final reaction products (Fig. 14). Also the reflectance behavior of these products is impressionable (Figs. 6b, 6d).

The following catechol-DAB medium is recommended:

- 25 mM HEPES/HEPSO-buffer, pH 8.0;
- 0.02% DAB and 0.005% catechol;
- (the addition of 0.005% TEMPO, dissolved in a small amount of tetrahydrofuran (THF), or of the better water soluble 4-carboxy-TEMPO, is possible leading to a distinct clearing up of the precipitation patterns);
- 0.001 - 0.01% hydrogenperoxide.

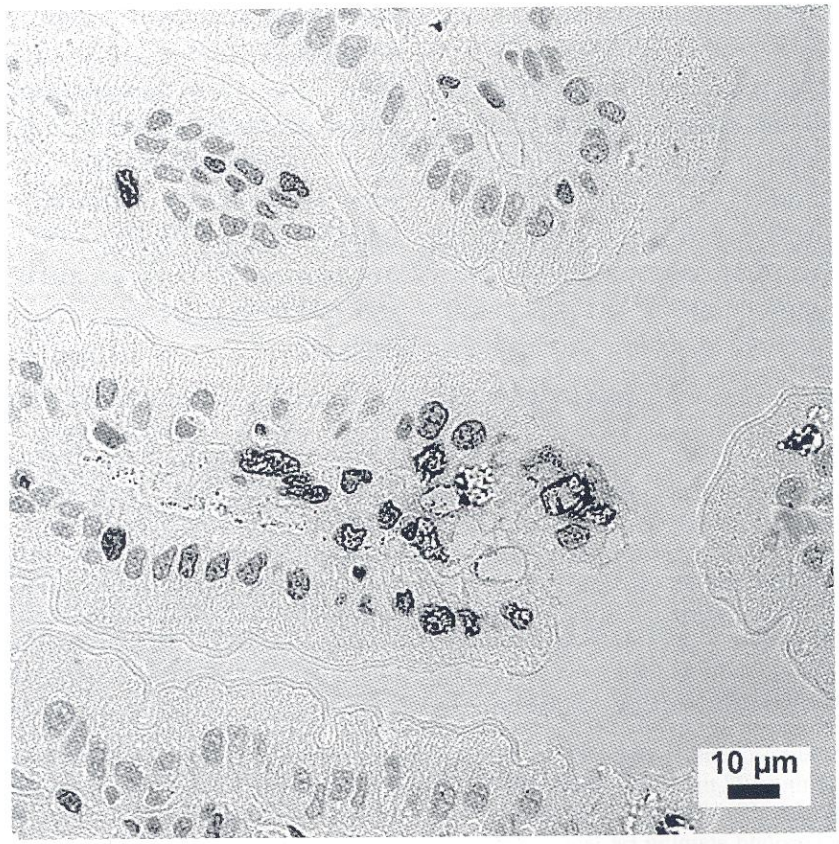

Fig. 14 *Immunobound peroxidase activity.* Apoptotic nuclei intestine, rat. TUNEL-reaction. Transmission image of PRP catechol-DAB polymers. Note the increased contrast and the high resolution power of the labelled nuclear structure of the apoptotoc nuclei at the tip of the villus. Semithin plastic section.

The incubation should carried out for 30 min. at 20°C.

In contrast, under the same conditions the additive 3,5-di-*tert*-butyl-catechol performed as an inhibitor (results have been omitted). This is due to the *tert*-butyl substituents preventing the occurrence of oxidative intermolecular crosslinkings subsequently only leading to radical trapping and 'oxidative power' consuming effects as well known from the action of some phenols as antioxidants (e.g. Wu and Lai, 1996).

For the explanation of the differing reddish-brownish colored reaction products of DAB in the presence of catechol as responsible side reaction must be taken into account the oxidative condenzation to phenazines (dibenzo-pyrazine derivatives) or oxazines of different molecular weights too, or the directly condenzation of the starting materials to 5H,10H-phenazines prior the oxidation reaction and their subsequently dehydrogenation. Both reactions give rise to a termination of the DAB oxidative polycondensation cascade (to polymeric phenazins) leading to more oligomeric products of lowered molecular weights and an overall mean hypsochromic absorption shift (Phenazines and oxazines as well as their hetero-analogeous thiazines are used as fluorescent dyes, some of these dyes are employed as laser dyes; Gerhartz, 1988; Van Duuren, 1963).

In an analogous manner to the above discussed 'catecholic termination effect', the possibility of controlling a narrowed polydispersity of the reaction products by other additives (phenols, amines, metal ions, stable radicals) is assumable, either in terms of nucleophilic/electrophilic interactions with quinoid intermediates or in terms of free radical processes.

The idea of the selective and reversible termination of 'living radical ends' with appropriate reagents led to 'living polymerization techniques', giving the chemist a powerful tool to achieve a high degree of control over polymer architecture (more recently reviews: Hawker, 1996; Webster, 1991; transition metal complexes: Sawamoto *et al.*, 1996). Surprisingly, kinetic stable nitroxyl radicals were successfully employed even in the entantioselec-

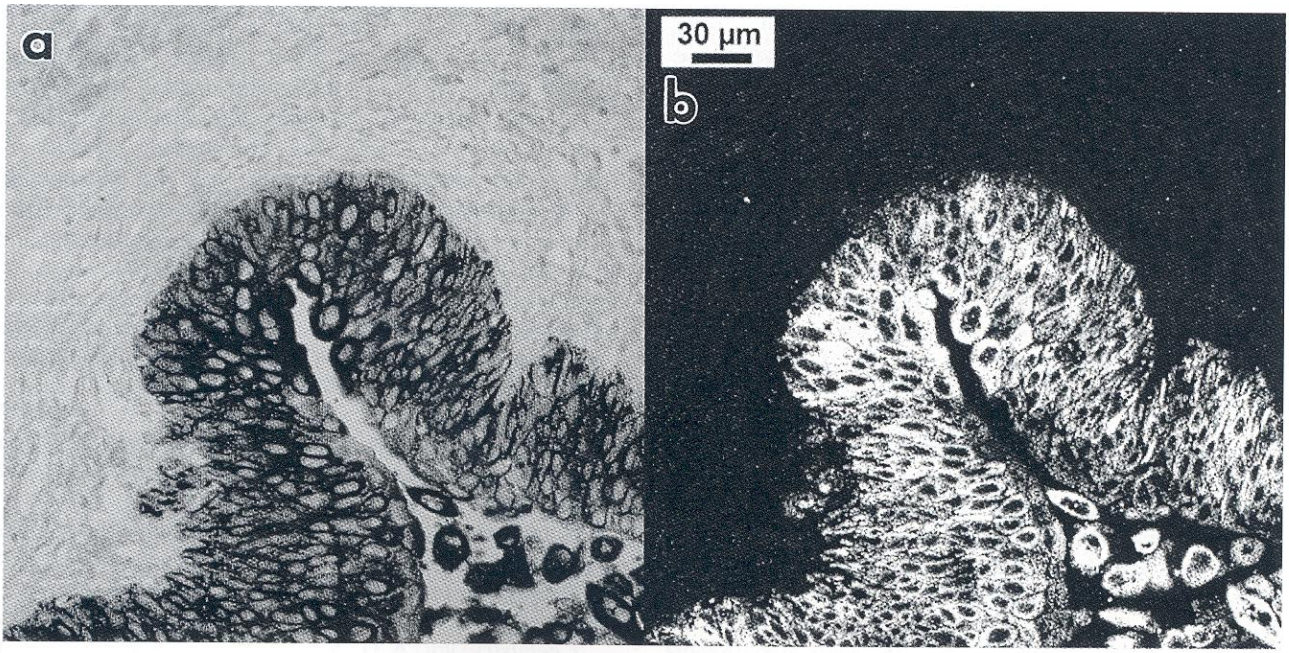

Fig. 15 *Immunobound peroxidase activity.* Cytokeratin within the urothelium of human ureter. Paraffin section. **a**) Transmission image; **b**) reflectance image of TEMPO-catechol-DAB polymers. Note the high transmission contrast, the high reflectance intensity as well as the high resolution of the reaction products in the cytokeratin structures.

tive organic synthesis (Braslau *et al.*, 1997).

Thus, we investigated the influence of some stable free nitroxyl-radicals utilized in 'living polymerizations' (TEMPO; its better water soluble 4-carboxylate and the analogue 3-carbamoyl-2,2,5,5-tetrametyl-3-pyrrolin-1-oxyl, results for the latter have been omitted because of its comparable overall effect), and exemplarily the radical mediator *meso*-tetraphenyl-porphine on the oxidation reaction of DAB. Details are compiled in table 2.

The laser transmission contrast was found to be improved slightly (also the reflection intensity!) when instead or in the presence of metal-additives the DAB polymerization is modified by using TEMPO or its analogues (Fig. 15).

OUTLOOK

In conclusion, the high-resolution detection of enzymatic activities in routine sections (vibratome, cryotome, semithin) using the reflectance or transmission mode of the CLSM or both in combination, especially in the Ce^{III}- to Ce^{IV}-based version, opens new possibilities for cellular and molecular biological studies. The techniques may be a valuable tool for basic research as well as for clinical diagnosis.

Acknowledgments – The authors wish to thank Mrs. U. Möller, Mrs. S. Hitschke and Mrs. E. Günther for excellent technical assistance as well as Mrs. G. Hofmann for her care in preparing the manuscript.

REFERENCES

Abubaker, M.A., Harrington, K. and Wandruszka, R., Fluorescence sensitization of aqueous terbium and europium ions without aromatic donors or synergistic agents. *Anal. Lett.* 1993, **26**: 1681-1692.

Arnold, N., Seible, R., Kessler, C. and Wienberg, J., Nonradioactive *in situ* hybridization with digoxigenin-labelled DNA probes. *Biotech. Histochem.* 1992, **67**: 59-67.

Aschoff, A.P. and Jirikowski, G.F., Apoptosis: Correlation of cytological changes with biochemical markers in hormone dependent tissues. *Horm. Metabol. Res.* 1997, **29**: 535-543.

Bendayan, M., Ultrastructural localization of nucleic acids by the use of enzyme-gold complexes. *J. Histochem. Cytochem.* 1981, **29**: 531-541.

Braslau, R., Burrill, L.C., Mahal, L.K. and Wedeking, T., Ein völlig radikaler Zugang zur Stereoselektivitätskontrolle: Kupplung von prochiralen radikalen mit chiralen Nitroxylradikalen. *Angew. Chem.* 1997, **109**: 247-249.

Brook, M.A., Casstle, L., Smith, R.L., Higgins, R. and Morris, K.P., Aromatic hydroxylation. Part 7. Oxidation of some benzoid compounds by iron compounds and hydrogen peroxide with the aromatic compound acting as substrate and solvent. *J. Chem. Soc. (Perk. Trans. 2:)* 1982, 687-692.

Cheng, P.C. and Summers R.G., Image contrast in confocal light microscopy. In: *The Handbook of biological confocal Light Microscopy*, Pawley, J. (ed.), IMR Press, Madison, 1988, pp. 163-179.

Condreau, M.A., Schwendener, R.A., Niederer, P. and Anliker, M., Time-resolved flow cytometry for the measurement of lanthanide chelate fluorescence. I. Concept and theoretical evaluation. *Cytometry* 1994, **16**: 187-194.

Coulombe, P.A., Kan, F.W.K. and Bendayan, M., Introduction of a high-resolution cytochemical method for studying the distribution of phospholipids in biological tissues. *Eur. J. Cell. Biol.* 1988, **46**: 564-576.

Cuello, A.C., Immunohistochemistry. John Wiley, Chichester, 1983.

Deitch, J.S., Smith, K.L., Swann, J.W. and Turner, J.N., Parameters affecting imaging of the horseradish-peroxidase-diaminobenzidine reaction product in the confocal scanning laser microscope. *J. Microsc.* 1990, **160**: 265-278.

Deitch, J.S., Smith, K.L., Lee, C.L., Swann, J.W. and Turner, J.N., Confocal scanning laser microscope images of the hippocampal neurons intracellularly labeled with biocytin. *J. Neurosci. Meth.* 1990, **33**: 61-76.

Deitch, J.S., Smith, K.L., Swann, J.W. and Turner, J.N., Ultrastructural investigation of neurons identified and localized using the confocal scanning laser microscope. *J. Electron. Microsc. Tech.* 1991, **18**: 82-90.

Doucet, J.P., Murpy, B.J. and Tuana, B.S., Modification of a discontinuous and highly porous sodium dodecylsulfate-polyacrylamide gel system for minigel electrophoresis. *Anal. Biochem.* 1990, **190**: 209-211.

Doucet, J.P. and Trifaro, J.M., A discontinuous and highly porous sodium dodecylsulfate-polyacrylamide slab gel system of high resolution. *Anal. Biochem.* 1988, **168**: 265-271.

Duschner, H., Konfokale Laser-Scanning-Mikroskopie (CLSM) - ein neues Verfahren zur Beurteilung von Zahnschmelzstrukturen. *Dental Forum* 1995, **1**: 3-7.

Gerhartz, W., (ed.) *Ullmann's Encyclopedia of industrial Chemistry*, vol. **A 11**, VCH Weinheim, 5th ed., 1988, p. 284.

Gu, M. and Sheppard, C.J.R., Experimental investigation of fibre-optical confocal scanning microscopy: Including a

comparison with pinhole detection. *Micron* 1993, **24**: 557-565.

Gütlich, P. and Dei, A., Valenztautomerie mit spontanem Spinübergang in Übergangsmetal-1,2-Benzochinon-Komplexen. *Angew. Chem.* 1997, **109**: 2852-2855.

Halbhuber, K.-J., Feuerstein, H., Zimmermann, N., Klinger, M., Kalicharan, D. and Hupfer, U., Improved light microscopic-demonstration of D-amino acid oxidase activity in cryotome sections using cerium ions as capturing and amplifying agent - the Ce/Ce-H_2O_2-DAB procedure. *Cell. mol. Biol.* 1991, **37**: 279-294.

Halbhuber, K.-J., Schulze, M., Rhode, H., Bublitz, R., Feuerstein, H., Walter, M., Linss, W., Meyer, H.W. and Horn, A., Is the brush border membrane of the intestinal mucosa a generator of "chymosomes"? *Cell. mol. Biol.* 1994, **40**: 1077-1096.

Halbhuber, K.-J., Scheven, Ch., Jirikowski, G., Feuerstein, H. and Ott, U., Reflectance enzyme histochemistry (REH): visualization of cerium-based and DAB primary reaction products of phosphatases and oxidases in cryostat sections by confocal laser scanning microscopy. *Histochem. Cell Biol.* 1996, **105**: 239-249.

Ito, Y. and Otsuki, Y., Localization of apoptotic cells in the human epidermis by an *in situ* DNA nick end-labeling method using confocal reflectant laser microscopy. *J. Histochem. Cytochem.* 1998, **46**: 783-786.

Hardonk, M.J., Dijkhuis, F.W.J., Haarsma, T.J., Koudstaal, J. and Huijbers, W.A.R., Application of enzyme histochemical methods to isolated subcellular fractions and to sucrose-ficoll density gradients. A contribution to the comparison of histochemical and biochemical data. *Histochemistry* 1977, **53**: 165-181.

Hawker, C.J., Advances in "living" free-radical polymerization: Architectural and structural control. *Trends Polymeer Sci.* 1996, **4**: 183-188.

Hiraoka, T., Hirai, K.I. and Ueda, T., Cobalt acetylacetonate-diaminobenzidine reaction for microspectrophotometry of cytochrome oxidase. *Acta Histochem. Cytochem.* 1986, **19**: 429-436.

Hulstaert, C.E., Kalicharan, D. and Hardonk, M.J., Cytochemical demonstration of phosphatases with the cerium method. In: *Techniques in diagnostic Pathology,* vol. **1**, Bullock, G.R., Leathem, A.G. and van Velzen, D. (eds.), Acad. Press, San Diego, 1989, pp. 133-150.

Kazama, J.J., Aikata, T., Arakawa, M. and Ozawa, H., A new histochemical double-stain method using three-dimensional analysis with confocal laser scanning microscopy. *Biotech. Histochem.* 1994, **69**: 324-328.

Landegent, J.E., *In situ Hybridization using 2-Acetylamino-Fluorene-modified nucleic Acid Probes. Doctor Thesis.* K&L Grafische Producties, Amsterdam, 1987.

Lempers, H.E.B., Ripolles, I., Garcia, A. and Sheldon, R.A., Metal-catalyzed oxidations with pinane hydroperoxide: a mechanistic probe to distinguish between oxometal and peroxometal pathways. *J. Org. Chem.* 1998, **63**: 1408-1413.

Lewis, D.E., Minshall, M., Wray, N.P., Paddock, S.W., Smith, L.C. and Crane, M.M., Confocal microscopic detection of human immunodeficiency virus RNA-producing cells. *J. infect. Dis.* 1990, **162**: 1373-1378.

Linares-Cruz, G., Millot, G., De Cremoux, P., Vassy, J., Olofsson, B., Rigaut, J.P. and Calvo, F., Combined analysis of *in situ* hybridization, cell cycle and structural markers using reflectance and immunofluorescence confocal microscopy. *Histochem. J.* 1995, **27**: 15-23.

Linares-Cruz, G., Rigaut, J.P., Vassy, J., De Oliveira, T.C., De Cremoux, P., Olofsson, B. and Calvo, F., Reflectance *in situ* hybridization (RISH): Detection, by confocal reflectance laser microscopy, of gold-labeled riboprobes in breast cancer cell lines and histological specimens. *J. Microsc.* 1994, **173**: 27-38.

Lojda, Z., Gossrau, R. and Schiebler, T.H., *Enzyme Histochemistry. A Laboratory Manual.* Springer Verlag, Berlin, 1979.

Luppa, H., Ambrosius, H. and Storch, W., Immunreaktionen in der Histochemie. In: *Handbuch der Histochemie,* vol. **IV/2** *Proteine*, Graumann, W. and Neumann, K. (eds.), Fischer, Stuttgart, 1986, pp. 1-418.

Meijer, A.E.F.H., Zur Histochemie der Enzyme. *Acta Histochem* 1975, Suppl. **XIV**: 33-44.

Neri, L.M., Cinti, C., Santi, S., Marchisio, M., Capitani, S. and Maraldi, N.M., Enhanced resolution of specific chromosome and nuclear regions by reflectance laser scanning confocal microscopy. *Histochem. Cell Biol.* 1997, **107**: 97-104.

Ott, U., *Enzymatische Untersuchungen zur endogenen Aktivität der alkalischen Phosphatase in der Darmschleimhaut der Ratte.* Dissertation FSU Jena, 1998.

Paddock, S., Mahoney, S., Minshall, M., Smith, L., Duvic, M. and Lewis, D., Improved detection of *in situ* hybridization by laser scanning confocal microscopy. *Biotechniques* 1991, **2**: 486-493.

Ploton, D., Gilbert, N., Ménager, M., Kaplan, H. and Adnet, J.J., Three-dimensional colocalization of nuclear argyrophilic components and DNA in cell nuclei by confocal microscopy. *J. Histochem. Cytochem.* 1994, **42**: 137-148.

Pluta, M., Reflection contrast microscopy. In: *Advanced Light Microscopy*: *Specialized Methods,* vol. **2**, Pluta, M. (ed.), Elsevier, Amsterdam, 1989, pp. 199-210.

Polak, J.M. and van Noorden, S., *Immunocytochemistry. Practical Applications in Pathology and Biology.* Wright - PSG, Boston, 1983.

Polak, J.M. and Varndell, I.M., *Immunolabeling for Electron Microscopy*. Elsevier, Amsterdam, 1984.

Rath, F.W., *Praktisch-diagnostische Enzymhistochemie.* Fischer, Jena, 1981.

Rawlins, D.J. and Shaw, P.J., *In situ* hybridization with digoxygenin-labelled probes and 1 nm gold conjugated antibodies with confocal optical sectioning and image reconstruction to describe the 3D arrangement of rDNA in intact plant tissue. In: *Trans R. Microsc Soc*, vol. **1**, Elder, H.Y. (ed.), Adam Hilger, Bristol, 1990, pp. 675-678.

Rigaut, J.P., Linares, G., Vassy, J., Downs, A.M., De Oliveira, T.C., De Cremoux, P. and Calvo, F., Reflectance *in situ* hybridization (RISH) - 3D confocal laser imaging and quantitation after immunogold labeling of a riboprobe.

Cytometry 1993, Suppl. **6**: p. 22.

Robinson, J.M. and Batten, B.E., Detection of cytochemical reactions using scanning laser confocal reflectance microscopy. *J. Cell Biol.* 1989a, **109**: 308a.

Robinson, J.M. and Batten, B.E., Localization of cytochemical reactions by scanning-laser confocal microscopy with the reflectance mode. *J. Histochem. Cytochem.* 1989b, **37**: 940.

Robinson, J.M. and Batten, B.E., Detection of diaminobenzidine reactions using scanning laser confocal reflectance microscopy. *J. Histochem. Cytochem.* 1989c, **37**: 1758.

Robinson, J.M. and Batten, B.E., Localization of cerium-based reaction products by scanning laser reflectance confocal microscopy. *J. Histochem. Cytochem.* 1990, **38**: 315-318.

Sawamoto, M. and Kamigaito, M., Living radical polymerizations based on transition metal complexes. *Trends Polymer Sci.* 1996, **4**: 371-376.

Sebastian, P. and Bock, R., Über die Anwendung der Dunkelfeldmikroskopie zur Beobachtung spezifisch gefärbter Strukturen in histologischen Schnitten. Leitz Mitt. Techn. Bd IX, Nr. 2, Wetzlar, 1987, pp. 53-58.

Seno, S., Akita, M. and Hsueh, C.L., A new method of the immunohistochemical detection of cellular antigens for light and electron microscopy. *Histochemistry* 1989, **91**: 449-454.

Seveus, L., Vaisala, M., Syrjanen, S., Sandberg, M., Kuusisto, A., Harju, R., Salo, J., Hemmila, I., Kojola, H. and Soini, E., Time-resolved fluorescence imaging of europium chelate label in immunhistochemistry and *in situ* hybridization. *Cytometry* 1992, **13**: 329-338.

Shotton, D.M., Electronic light microscopy: present capabilities and future prospects. *Histochem. Cell Biol.* 1995, **104**: 97-137.

Turner, J.N., Swann, J.W., Szarowski, D.H., Smith, K.L., Carpenter, D.O. and Fexjtl, M., Three-dimensional confocal light microscopy of neurons: fluorescent and reflection stains. In: *Cell biological Applications of confocal Microscopy. Methods in Cell Biology,* vol. **38**, Matsumoto, B. (ed.), Acad. Press, New York, 1993, pp. 345-366.

Van der Zee, J., Krootjes, B.B.H., Chingnell, C.F., Dubbelman, T.M.B.R. and van Steveninck, J., Hydroxyl radical generation by a light dependent *Fenton*-reaction. *Free Rad. Biol. Med.* 1993, **14**: 105-113.

Van Duuren, B.L., Effects of the environment on the fluorescence of aromatic compounds in solution. *Chem. Rev.* 1963, **63**: 325-354.

Van Noorden, C.J.F. and Frederiks, W.M., Cerium methods for light and electron microscopical histochemistry. *J. Microsc.* 1993, **171**: 3-16.

Van Noorden, C.J.F. and Hulstaert, C.E., Electron microscopical enzyme histochemistry. In: *Electron Microscopy in Biology. A practical Approach*, Chapter 6, Harris, R.J. (ed.), IRL Press, Oxford, UK, 1991.

Watanabe, M., Koide, T., Konishi, M., Kanbara, K. and Shimada, M., Use of confocal laser scanning microscopy in radioautographic study. *Cell. mol. Biol.* 1995, **41**: 131-136.

Webster, O.W., Living polymerization methods. *Science* 1991, **251**: 887-893.

Whallon, J.H., Preller, A. and Wilson, J. E., Reflection confocal imaging of type I and type III isozymes of hexokinase in PC12 cells. *Scanning* 1994, **16**: 111-117.

Wohlrab, R. and Gossrau, R., *Katalytische Enzym-histochemie. Grundlagen und Methoden für die Elektronenmikroskopie.* Fischer, Stuttgart, 1992, p. 264.

Wohlrab, F., Seidler, E. and Kunze, K.D., *Histo- und Zytochemie dehydrierender Enzyme.* Johann Ambrosius Barth, Leipzig, 1979.

Wu, Y.D. and Lai, K.W., A density functional study of substituent effects on the O-H and O-CH_3 bond dissoziation energies in phenol and anisole. *J. Org. Chem.* 1996, **61**: 7904-7910, and literature cited therein.